Electronic structure of aluminum nitride: Theory and experiment

S. Loughin and R. H. French
DuPont Co. Central Research, P.O. Box 80356, Wilmington, Delaware 19880

W. Y. Ching and Y. N. Xu
University of Missouri at Kansas City, Department of Physics, 1110 East 48th Street, Kansas City, Missouri 64110

G. A. Slack
General Electric Corporate Research & Development Center, 1 River Road, Schenectady, New York 12301

(Received 14 December 1992; accepted for publication 8 June 1993)

We report the results of a vacuum ultraviolet (VUV) study of single crystal and polycrystalline AlN over the range 4–40 eV and compare these with theoretical optical properties calculated from first principles using an orthogonalized linear combination of atomic orbitals in the local density approximation. The electronic structure of AlN has a two-dimensional (2D) character indicated by logarithmic divergences at 8.7 and 14 eV. These mark the centers of two sets of 2D critical points which are associated with N $2p \rightarrow$ Al $3s$ transitions and Al$=$N$\rightarrow$Al $3p$ transitions, respectively. A third feature is centered at 33 eV and associated with N $2s \rightarrow$ Al $3d$ transitions.

Recent efforts to develop electronic,[1] optical, and electro-optical[2-4] components and applications based on wide band-gap III-V materials have generated considerable practical interest in the electronic structure of AlN. While a number of theoretical calculations[5-10] of the band structure exist, the experimental work[11-14] available for comparison has been limited in either energy range or energy resolution. Extant experimental studies are mostly on thin films due to the difficulty of growing high-purity bulk crystals of AlN.

Aside from technological applications, the electronic structure of AlN is also of fundamental interest. Calculation of the electronic structure of ceramics is a developing area of theoretical physics and the nitrides are of particular importance because the bonding is more covalent than in the oxides. Experimental information about the electronic structure of AlN provides insight as to how theoretical models based on oxides should be adapted to covalent ceramics. Quantitative comparison of theory and experiment affords the best tool for gaining this insight. To this end, we present our results in terms of analytical critical point models of the interband transition strength, J_{cv}, for both a first principles calculation and a vacuum ultraviolet (VUV) optical measurement. Our method emphasizes the relationship among critical points grouping them into sets representative of transitions between pairs of bands, while other recent work[15] emphasizes individual critical points.

A single crystal (W201), with a thermal conductivity of 275 W m^{-1} K^{-1} grown by a modified Bridgman technique,[16] was studied. The oxygen content of the single crystal was 340 ppm, as previously reported.[18] Polishing with diamond powders suspended in high-purity dry kerosene yields an oxide-free surface for reflectance measurements. Oxidized surfaces give spurious results and were avoided by nonaqueous polishing. The polished face of the single crystal was near normal to the c axis.

The VUV reflectance spectra were obtained with a laser plasma sourced VUV spectrophotometer, described elsewhere.[9] Above the band gap at 6.2 eV, the spectra show two main features. A sharp peak appears at about 9 eV and a smaller, somewhat broader peak appears at about 14–15 eV. A small feature also appears at about 35 eV. Small features below the band gap are due to vacancies. The single crystal response was found to be representative of commercial polycrystalline substrates also studied.[17]

The spectrum was adjusted, consistent with an index of $n[1.25\ \text{eV}]=2.1$ A Kramers–Krönig (KK) analysis[20] recovered the phase information, $\theta[h\nu]$, and permitted calculation of other optical properties,[21] including the complex dielectric function shown in Fig. 1.

The energy band structure of AlN was calculated from first principles, using the orthogonalized linear combination of atomic orbitals (OLCAO) method with the local density approximation (LDA).[22] The resulting band dia-

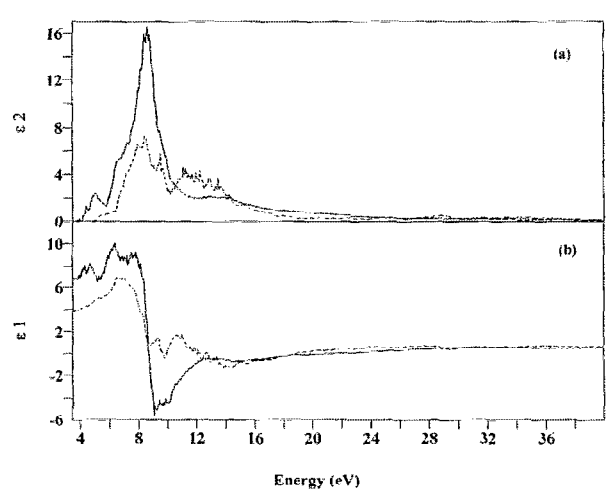

FIG. 1. The imaginary (a) and real (b) parts of the dielectric function for single crystal AlN with E⊥c (solid) are compared with those calculated from first principles for E⊥c (dashed).

 0003-6951/93/63(9)/1182/3/$6.00

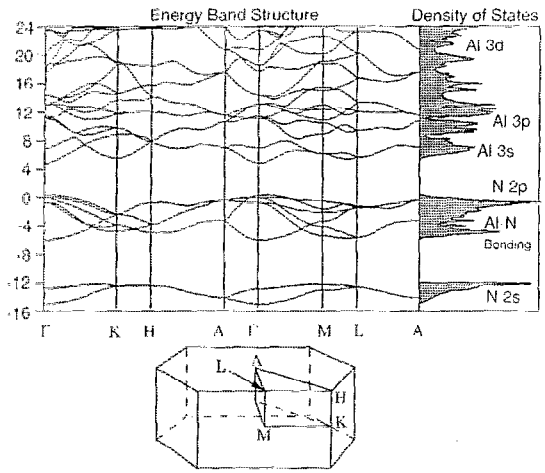

FIG. 2. The energy band structure of AlN is shown with the k-space directions referenced to the Brillouin zone as shown.

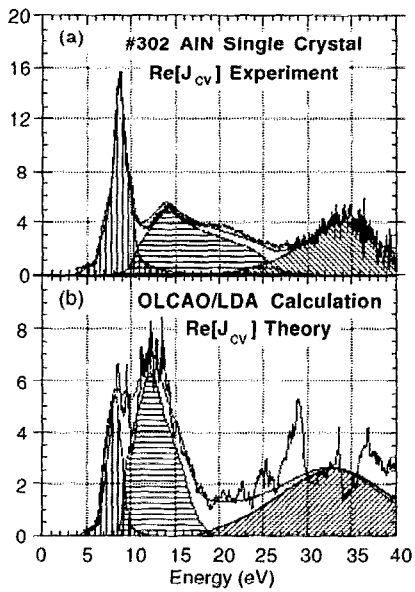

FIG. 3. The interband transition strength has been modeled using balanced sets of analytical critical point line shapes for both experiment (a) and theory (b).

gram and total density of states (DOS) are shown in Fig. 2.

The calculated band gap occurs at the zone center, E_0=4.5 eV. The conduction-band minimum at Γ has a simple parabolic shape in all three directions, however, the valence-band maximum is relatively flat in the Γ to K and Γ to M directions, but falls off sharply in the Γ to A direction. Thus, the hole effective mass, normalized to the rest mass of the electron, is nearly an order of magnitude larger in the basal plane (m^*=3.52 $\Gamma\rightarrow M$ and 3.40 $\Gamma\rightarrow K$) than in the c-axis direction (m^*=0.30 $\Gamma\rightarrow A$). As discussed by Nakao[23] such anisotropy in the bands leads to a reduction in the dimensionality of the optical response. Along with similar anisotropies occurring for other band pairings, this supports the possibility that features in the reflectance spectra are quasi-two dimensional.

The optical conductivity and matrix elements of momentum were evaluated[21,14] to determine the optical properties predicted by the first-principles calculation. The imaginary part of the dielectric function, $2\sigma/(h\nu)$, followed by KK analysis, yielded the complex dielectric function, $\varepsilon_1+i\varepsilon_2$, for E$\perp$**c**, as shown in Fig. 1.

With the experimental and theoretical results both in terms of the complex dielectric function, one can qualitatively compare the two. However, to gain further insight into how the differences relate to fundamental properties of the material requires a *quantitative* comparison, achieved through the use of analytical critical point models.[25–27] Unfortunately, the established approach of fitting the second derivative is difficult when the band structure and the experimental results are not well established, as is the case for most ceramics. We therefore fit the spectra using an *undifferentiated* model.[28] The interband transition strength J_{cv} is proportional to $(h\nu)^2\epsilon^2$. As with other optical properties, we can define a complex J_{cv} as

$$J_{cv}=\frac{m^2}{8\pi^2\hbar^2e^2}(h\nu)^2[\varepsilon_2+i\varepsilon_1]=\frac{m^2}{8\pi^2\hbar^2e^2}(h\nu)^2i\hat{\epsilon}^*, \quad (1)$$

where $\hat{\epsilon}$ is the usual complex dielectric function and the asterisk denotes complex conjugation. For computational convenience, we take the prefactor $(m^2\hbar^{-2}e^{-2})$ to be unity. The complex interband transition strength is then fit to

$$J_{cv}=i\left(C+(h\nu)^2-\sum_k A_k e^{i\phi_k}(h\nu-E_k+i\Gamma_k)^{n_k}\right)^*. \quad (2)$$

C is a complex constant, $h\nu$ is photon energy, and k indexes the critical points (CPs). The CP parameters are A_k, ϕ_k, E_k, Γ_k, and n_k, respectively identified as the amplitude, phase, energy, width, and dimensional exponent[26] for each critical point. Individual critical points are grouped into sets corresponding to transitions between a valence- and conduction-band pair. Transitions between a valence and a conduction band have well defined energies for the onset and exhaustion of transition strength. By demanding that Re[J_{cv}] arising from each set is asymptotic to zero at energies well outside the range of the set, we constrain the model to physically realistic, *balanced sets* of CPs.

Figure 3 shows the models constructed using Levenberg–Marquardt optimization for the E$\perp$**c** J_{cv}, both as measured VUV and as calculated OLCAO/LDA. The parameters for these models are compared in Table I. Due to band splitting at the valence- and conduction-band edges, a double, overlapping set was used to model the low energy feature with a single saddle point.

Each of the critical points can be referenced to the band structure of AlN. The calculated band diagram indicates that AlN has a direct band gap occurring at the Γ point with an energy separation of 4.5 eV, which is considerably lower than the 6.3 eV found experimentally. However, LDA calculations generally give lower than observed values for the gap.

A two-dimensional CP has been assigned to the band gap, suggesting that the reduced effective mass is consid-

TABLE I. The fit parameters for the models of experiment and theory are compared. The models had a reduced χ^2 of 62, with $C=20.08+i1.34$ (experiment) χ^2 of 48, with $C=25.93+i1.87$ (theory).

Critical pt.	Energy (eV)		Width (eV)		Amplitude	
k/type	Expt.	Theory	Expt.	Theory	Expt.	Theory
$1/D_0$	6.29	4.69	0.38	0.31	1.32	0.11
$2/D_0$	8.02	6.86	0.38	0.31	3.17	1.21
$3/D_1$	8.68	8.54	0.38	0.31	4.45	1.32
$4/D_2$	9.16	9.10	0.38	0.31	2.32	0.29
$5/D_2$	10.39	9.87	0.38	0.31	2.18	1.07
$6/D_0$	10.22	9.24	0.78	0.30	1.16	1.23
$7/D_1$	14.00	12.31	0.78	0.78	1.08	1.91
$8/D_2$	25.67	16.87	1.84	1.18	0.99	1.14
$9/S_0$	33.85	33.03	5.64	10.0	26.13	36.2

erably different in one of the three directions. From the calculated band structure results, the reduced masses are $\mu_{\Gamma\to M}=0.36$, $\mu_{\Gamma\to K}=0.37$, and $\mu_{\Gamma\to A}=0.16$. So $\mu_{\Gamma\to A}$ is 43% of μ in the other directions. Table II presents a scheme for assigning the critical point energies to specific transitions where the majuscule labels the symmetry with reference to Fig. 2, and the subscripts index the set membership and type of critical point. Orbital origins, based on the partial DOS from the OLCAO/LDA calculation, aid in identifying the nature of transition typical of each set, although we recognize that they are not formally correct.

The optical response of single crystal AlN includes several prominent features which were resolved into three sets of balanced critical points. The first set ranges from the band gap at 6.3–10.4 eV, the point at which transitions between the upper valence band and lower conduction band are exhausted. The conventional direct gap fit of $\alpha^2(h\nu)^2$, with the absorption coefficient, α, calculated from the first set, gives a gap of 6.2 eV. Based on analysis of the orbital decomposition of the density of states, this set was attributed to transitions between N $2p$ to Al $3s$ states. These lower energy features have a quasi-two-dimensional character, which is suggested by the existence of a single sharp maximum in the optical response at 8.7 eV.

Above 10.2 eV, another set of features appears, which is also two dimensional in character, and includes an onset at 10.2 eV, a logarithmic divergent peak at 14.0 eV, and a broad interband maximum centered at 25.7 eV. This set is identified with transitions between Al=N bonding states and Al $3p$ antibonding states. A third set, at much higher energies, could not be resolved into discrete critical points and was modeled as a broad zero-dimensional feature at 33.8 eV, probably arising from N $2s$ to Al $3d$ transitions.

The optical response calculated from the LDA band structure was also resolved into three sets of balanced critical points. Using the same orbital character assignments, the predicted energies for the N $2p$ to Al $3s$ set of transitions agreed closely with the experiment, except at the band gap. The energies for the Al=N to Al $3p$ set of transitions were lower than experimental values by about 2 eV. The N $2s$ to Al $3d$ transitions did not appear as a coherent set, however, the calculated response did include transitions in this energy range.

TABLE II. Assignment of features in the electronic structure of AlN.

Energy (eV)	Type	Assignment	Interband Δ(eV)	Predominant orbital character
6.3	D_0	Γ_{01}	4.5	
8.0	D_0	Γ'_{01}	7.2	
8.7	D_1	A_{11}	9.9	N $2p\to$Al $3s$
9.2	D_2	H_{21}	11.5	
10.4	D_2	H'_{21}	12.5	
10.2	D_0	A_{02}	11.1	
14.0	D_1	Γ_{12}	13.2	Al=N$\to$Al $3p$
25.7	D_2	H_{22}	19	
33.9	S_0	Γ_{03}	27–37	N $2p\to$Al $3d$

The authors are grateful for the assistance of D. J. Jones at DuPont, D. N. Elliott at Martin Marietta, and to the U. S. Department of Energy for funding the theoretical calculations under Grant No. DE-FG02-84ER45170.

[1] W. J. Meng, D. T. Morelli, D. M. Roessler, and J. Heremans, J. Appl. Phys. **69**, 846 (1991).
[2] W. R. L. Lambrecht and B. Seagall, Phys. Rev. B **43**, 7070 (1991).
[3] T. Ohta, K. Inoue, M. Uchida, K. Yoshioka, T. Akiyama, S. Furukawa, K. Nagata, and S. Nakamura, Jpn. J. Appl. Phys. **28**, 123 (1989).
[4] C. R. Aita, J. G. Kubiak, and F. Y. H. Shih, J. Appl. Phys. **66**, 4360 (1989).
[5] B. Hejda and K. Hauptmanová, Phys. Status Solidi **36**, K95 (1969).
[6] S. Bloom, J. Phys. Chem. Solids **32**, 2027 (1971).
[7] A. Kobayashi, O. F. Sankey, S. M. Volz, and J. D. Dow, Phys. Rev. B **28**, 935 (1983).
[8] M. Z. Huang and W. Y. Ching, J. Phys. Chem. Solids **46**, 977 (1985).
[9] D. Jones and A. H. Lettington, Solid State Commun. **11**, 701 (1972).
[10] W. Y. Ching and B. N. Harmon, Phys. Rev. B **34**, 5305 (1986).
[11] V. N. Meleshkin, V. V. Mikhailin, V. E. Oranovskii, P. A. Orekhanov, I. Pastrnák, S. Pacesova, A. S. Salamatov, M. V. Fok, and A. S. Yarov, in *Synchrotron Radiation*, edited by N. G. Basov (Lebendev Physics Institute, Moscow, 1975), pp. 169–174.
[12] H. Yamashita, K. Fukui, S. Misawa, and S. Yoshida, J. Appl. Phys. **50**, 896 (1979).
[13] C. G. Olson, J. H. Sexton, D. W. Lynch, A. J. Bevolo, H. R. Shanks, B. N. Harmon, W. Y. Ching, and D. M. Wieliczka, Solid State Commun. **56**, 35 (1985).
[14] M. Gautier, J. P. Duraud, and C. LeGressus, J. Appl. Phys. **61**, 574 (1987).
[15] C. C. Kim, J. W. Garland, H. Abad, and P. M. Racah, Phys. Rev. B **45**, 11749 (1992).
[16] G. A. Slack and T. F. McNelly, J. Cryst. Growth **34**, 263 (1976); G. A. Slack and T. F. McNelly, *ibid.* **42**, 560 (1977).
[17] Courtesy of J. B. Blum, CeraTronics-Toshiba, 112 Turnpike Road, Westboro, MA 01581
[18] G. A. Slack, R. A. Tanzilli, R. O. Pohl, J. W. Vandersande, J. Phys. Chem. Solids **48**, 641 (1987).
[19] R. H. French, Phys. Scri. **41**, 404 (1990).
[20] M. L. Bortz and R. H. French, Appl. Spectrosc. **43**, 1498 (1989).
[21] cf. F. Wooten, *Optical Properties of Solids* (Academic, San Diego, 1972).
[22] W. Y. Ching, J. Am. Ceram. Soc. **73**, 3135 (1990).
[23] K. Nakao, J. Phys. Soc. Jpn. **25**, 1343 (1968).
[24] G. Gilat and N. R. Bharatiya, Phys. Rev. B **12**, 3469 (1975).
[25] M. Cardona, *Solid State Physics, Advances in Research and Applications*, edited by F. Seitz, D. Turnbull, and H. Ehrenreich (Academic, New York, 1969), pp. 15–25.
[26] D. E. Aspnes, writing in *Handbook on Semiconductors, Volume 2, Optical Properties of Solids*, edited by T. S. Moss and M. Balkanski (North-Holland, Amsterdam, 1980), pp. 123–133.
[27] D. W. Lynch, in *Handbook of Optical Constants of Solids*, edited by E. D. Palik (Academic, Orlando, FL, 1985), pp. 190–211.
[28] S. Loughin, Ph. D. dissestation, University of Pennsylvania, pp. 61–93, Ann Arbor MI, UMI Accession No. 9227713 (1992).